AD_____

Award Number: W81XWH-10-1-0766

TITLE: Computational Model of the Eye for Primary and Secondary Blast Trauma

PRINCIPAL INVESTIGATOR: Dr. Thao Nguyen

CONTRACTING ORGANIZATION: Johns Hopkins University Applied Physics
Laurel, MD 20723

REPORT DATE: October 2011

TYPE OF REPORT: Annual

PREPARED FOR: U.S. Army Medical Research and Materiel Command
Fort Detrick, Maryland 21702-5012

REPORT DOCUMENTATION PAGE

Form Approved
OMB No. 0704-0188

1. REPORT DATE *(DD-MM-YYYY)*	**2. REPORT TYPE**	**3. DATES COVERED** *(From - To)*
01-10-2011	Annual	28 Sep 2010 - 27 Sep 2011

4. TITLE AND SUBTITLE
Computational Model of the Eye for Primary and Secondary Blast Trauma

5a. CONTRACT NUMBER

5b. GRANT NUMBER
W81XWH-10-1-0766

5c. PROGRAM ELEMENT NUMBER

6. AUTHOR(S)
Dr. Thao Nguyen

E-Mail: vicky.nguyen@jhu.edu

5d. PROJECT NUMBER

5e. TASK NUMBER

5f. WORK UNIT NUMBER

7. PERFORMING ORGANIZATION NAME(S) AND ADDRESS(ES)
Johns Hopkins University Applied Physics
Laurel, MD 20723

8. PERFORMING ORGANIZATION REPORT NUMBER

9. SPONSORING / MONITORING AGENCY NAME(S) AND ADDRESS(ES)
U.S. Army Medical Research and Materiel Command
Fort Detrick, Maryland 21702-5012

10. SPONSOR/MONITOR'S ACRONYM(S)

11. SPONSOR/MONITOR'S REPORT NUMBER(S)

12. DISTRIBUTION / AVAILABILITY STATEMENT
Approved for Public Release; Distribution Unlimited

13. SUPPLEMENTARY NOTES

14. ABSTRACT

This report describes the FY11 research accomplishments and their significance. In this first year of the project, we focused on developing the experimental and modeling tools for an innovative dynamic inflation test method for characterizing the stress-strain response and rupture conditions of the tissue of the eye-wall under blast conditions. Specifically, we designed and built a shock tube test system and began developing a constitutive model for the stress-strain response of the cornea and sclera that incorporates the anisotropic collagen lamellar structure. The shock-tube test system and constitutive model will be used in FY12 to measure the dynamic stress-strain response and rupture conditions of human cornea and sclera, and to develop a finite element model of the globe that features detailed of the microstructure and macrostructure of the cornea and sclera. We have made significant progress towards Specific Aim 1 of the project, which is to characterize the high-rate anisotropic stress response of the cornea and sclera, and Specific Aim 3, which is to develop a computational model of the eye in the human head.

15. SUBJECT TERMS
dynamic inflation, shock tube system, digital image correlation, microstructure-based constitutive model, cornea, sclera, anisotropy

16. SECURITY CLASSIFICATION OF:			**17. LIMITATION OF ABSTRACT**	**18. NUMBER OF PAGES**	**19a. NAME OF RESPONSIBLE PERSON**
a. REPORT	**b. ABSTRACT**	**c. THIS PAGE**			USAMRMC
U	U	U	UU	19	**19b. TELEPHONE NUMBER** *(include area code)*

Table of Contents

1.0 INTRODUCTION

The overall goal of this project is to develop an experimentally validated computational model of the eye and apply the model to evaluate the stresses and deformations incurred by the eye-wall and critical ocular components from blast overpressures, and to investigate the interaction between the standard issue eye protection and the blast wave, as well as its effect on the mechanical loading of the eye. The model will be developed based on the following working hypotheses.

1) The anisotropic mechanical properties of the cornea and sclera as derived from the collagen structure are critical to modeling the interaction of the blast wave and the globe. 2) The mechanical behavior of the cornea and sclera under dynamic (high-rate) loading is significantly different than under quasi-static (slow-rate) loading. 3) The surrounding environment of the globe, including the extra-ocular tissues of the orbit and the skull is important to modeling injuries to the eye from blast and fragments. In this first year of the project, we focused on designing and building the shock tube test system and developing a stress-strain model for the cornea and sclera that incorporates the anisotropic collagen lamellar structure. We have made significant progress towards Specific Aim 1 of the project, which is to characterize the high-rate anisotropic stress response of the cornea and sclera, and Specific Aim 3, which is to develop a computational model of the eye in the human head.

2.0 BODY

2.1 Dynamic Inflation Experiments

To understand ocular blast injuries, the behavior of ocular tissues under high pressures and at high loading rates needs to be measured and understood. The behavior of ocular tissues is anisotropic and non-uniform owing to the preferential collagen fibril arrangement in these tissues. We designed and built a shock tube setup coupled with full field displacement measurements in FY11. The shock tube experimental apparatus will be applied to perform dynamic inflation experiments to characterize the regionally varying stress-strain and failure response of the eye-wall and to characterize the response of the globe to shock loading characteristics of

primary blast conditions. The idea behind the dynamic inflation experiments is to record the dynamic pressure and full field displacement history at various levels of pressure. The following subsections describe the design and calibration of the shock tube, and a preliminary test on bovine cornea.

2.1.1 Design and construction of shock tube:

Figure 1 shows the schematic of the shock tube setup for dynamic inflation experiments. The shock tube, a specimen holding fixture and 2 high-speed imaging cameras are the components of the setup.

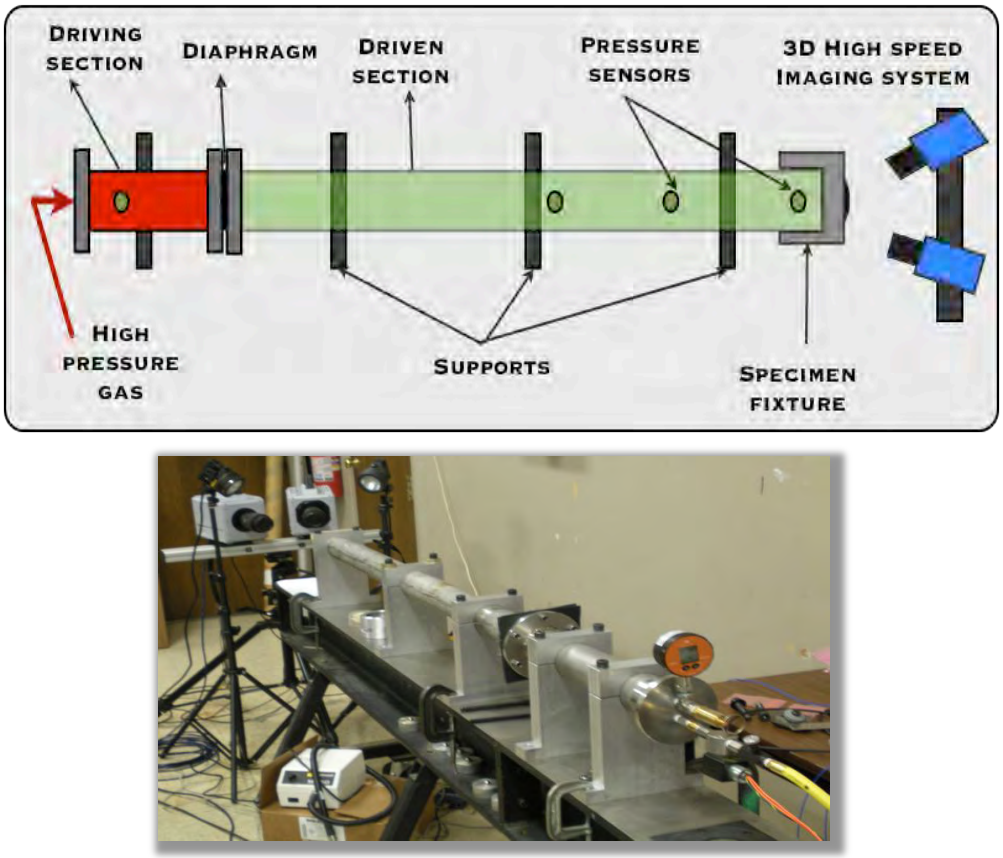

Figure 1: (Top) Schematic of a shock tube setup for dynamic inflation experiment. (Bottom) Actual shock tube setup.

A shock tube is a long tube device consisting of a high-pressure gas section (driving section) and a low-pressure gas section (driven section) separated by a diaphragm. The diaphragm is mechanically ruptured to generate a shock wave that travels away

from the diaphragm towards the end of the driven section. The ocular tissue, fixed at the end of the driven section will then dynamically inflate under high pressure (the pressure behind the shock wave) and high loading rates. The dynamic pressure and full field displacement history is recorded at various levels of pressure to study different properties such as the rate effects and anisotropy in the tissue.

The pressure profiles along the length of the shock tube before and after rupture of the diaphragm and the wave propagation in the tube are shown in the figure below. The design principles of a shock tube are described in detail in [1].
In designing the tube, lengths of the driving and the driven section and diameter of the tube are the important design parameters. Other elements such as thickness of the tube, supports, and endplates are designed from simple design calculations. Space availability in the laboratory determines the total length of the tube. An arbitrary driven section length is chosen. The driving section length is then calculated from the driven section length using the fact that a particular combination of driving and driven section length gives an approximately constant pressure pulse width for a range of pressures in different experiments. It should be noted that different driving sections could be used with a single driven section to produce different pulse widths in an experiment. The diameter of the tube is decided using the fact that the driven section length of the tube has to be at least 20 times the diameter of the tube. This is because after the diaphragm ruptures it takes some distance before a planar shock wave is established. The final dimensions of the tube are: tube diameter of 2.5", driving section length of 18", driven section length of 60". The shock tube is instrumented with: 3 PCB Piezotronics dynamic pressure sensors (model 102B16) with resonant frequency ~500 kHz at 25, 50, and 57 inches from the specimen to record the dynamic pressure history, and 2 Photron SA 5 cameras, with frame rates of 87,500 fps and 256 X 256 pixel resolution to image the deforming surface for digital image correlation (DIC).

2.1.2 Validation of shock tube setup and DIC displacement measurements:

We validated the design of the shock tube and the accuracy of the DIC displacement measurements prior to experimental testing. The shock tube design

was validated by comparing the pressure measurements with the theoretical values calculated from the shock tube dimensions. Using a 0.0005" thick PET (Polyethylene terephthalate) membrane as a diaphragm, dynamic pressure history was recorded at the three pressure sensors in the driven section of the tube for several experiments. Typical data from these experiments is shown in Figure 2.

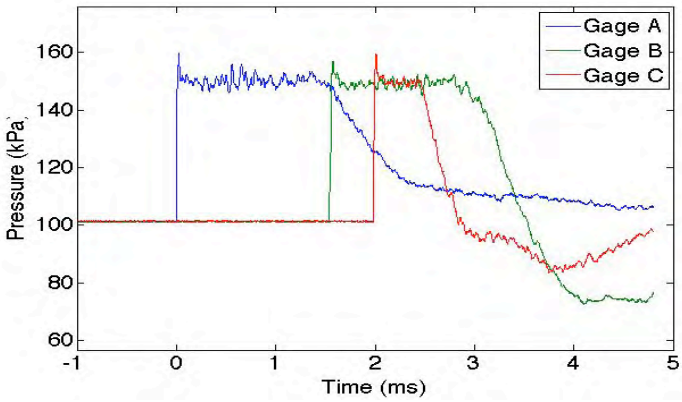

Figure 2: Typical dynamic pressure history obtained in a shock tube experiment.

The shock wave speed was calculated from the distance between two pressure gages and the travel time of the wave between the two gages. From the wave speed, the theoretical pressure behind the shock wave was calculated using,

$$\frac{p_2}{p_1} = \frac{2\gamma M^2 - (\gamma - 1)}{\gamma + 1} \qquad (1)$$

where, p_1 is the pressure of the gas in the driven section (usually Atmospheric pressure), p_2 is the pressure of the gas behind the shock wave, γ is the ratio of specific heats of the gas in driven section of the tube and M is the Mach number, or the strength of the shock wave (given as the ratio of wave speed to speed of sound). It is then compared to the pressure obtained by the pressure gages. The results in Table 1 showed good agreement between theoretical and observed pressures. The deviation of 10-12 kPa between theoretical and observed pressures is consistent throughout and indicates energy lost in friction as well as in the diaphragm rupture, which is not considered in the theoretical formulation. Also, the tests from equal thickness diaphragm material were as shown by the results for test 2 to 5.

Test No.	Diaphragm Material	Shock wave speed (m/s)	Shock Strength	Pressure behind shock wave (kPa)	
				Theoretical	Observed
1	Al foil	381	1.150	139.5	126
2	PET	398	1.202	153.8	141
3	PET	402	1.214	157.2	145
4	PET	405	1.223	159.8	146
5	PET	415	1.253	168.6	152
6	PET	423	1.277	175.9	164

Table 1: Theoretical and observed pressure comparison from shock tube experiments

The displacement measurements in a dynamic inflation experiment are measured by the non-contact measurement technique of DIC [2]. This technique is widely validated in literature for 2D applications, comparing the DIC displacement measurements with other contact displacement measurement techniques such as strain gages, LVDT's [3,4]. We designed and performed a validation test for the 3D (stereoscopic) DIC measurement for the quasi-static inflation test setup described in [5] and the shock tube-inflation test setup. The results of the validation in the in-plane (image plane) and out-of-plane displacement measurements are shown in Fig. 3 for the quasi-static inflation apparatus.

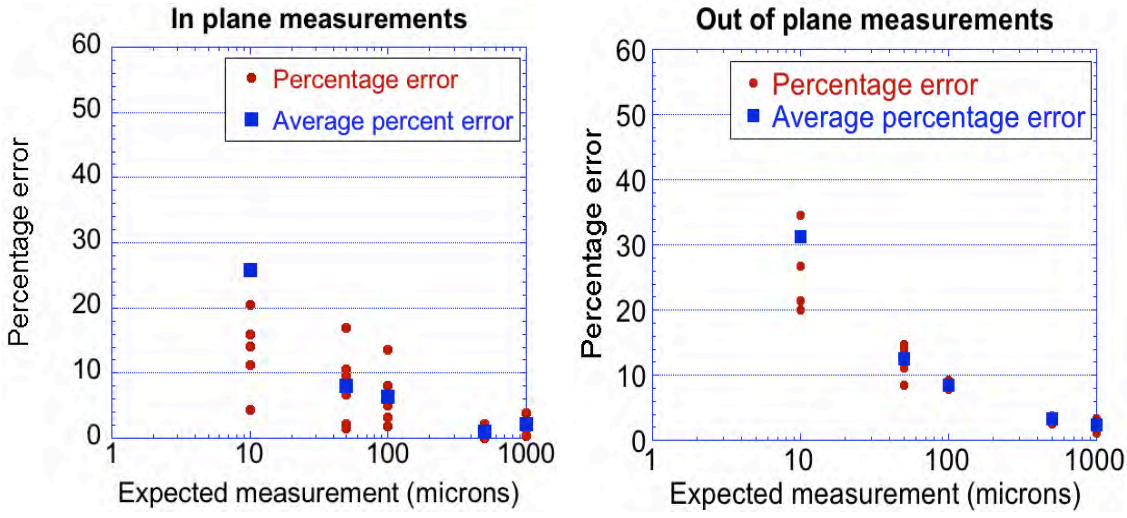

Figure 3: 3D DIC displacement measurement validation results for quasi-static inflation setup.

A translation stage with 3 degrees of freedom controlled with a micrometer screw gauge with a resolution of 2 microns to move along the x and y axes and with a picomotor with a resolution of 28nm to move along the z axis was used to validate these measurements. A random speckle pattern was applied on a ping-pong ball that was firmly fixed to the stage. The stage was moved a specific prescribed distance (10 microns, 50 microns, 100 microns, 500 microns and 1 mm as shown in the above plots) and DIC was used to calculate the displacements point-wise over the speckled region. The difference between the prescribed displacements and DIC displacements was measured as the error in the DIC displacement measurements. From the plots it can be seen that the error reduced from about 30% at 10 micrometers to about 1-2% at 1 mm for both in-plane and out-of-plane directions. This error included the uncertainty in the prescribed displacement of the stage (2 microns, making up for 20% of the total error at 10 microns level). The results showed that measurements in both in- and out-of-plane directions can be made from 10 microns to 1 mm with an accuracy of 2 microns.

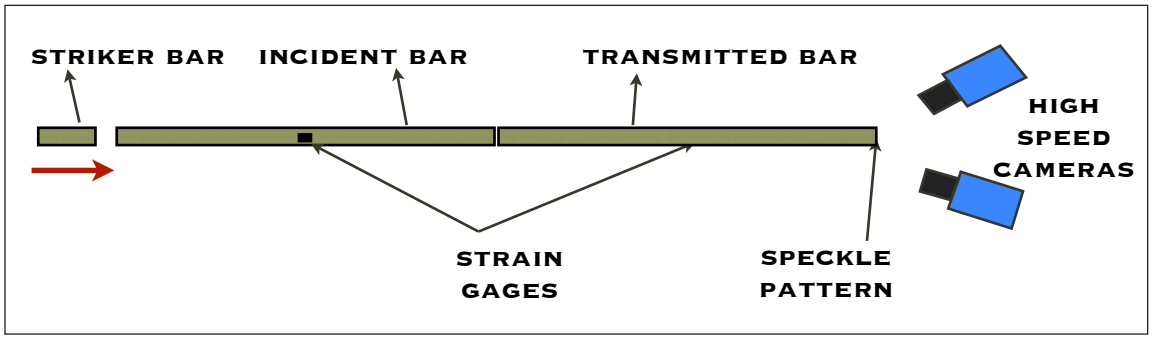

Figure 4: Schematic for the dynamic validation using Kolsky bars.

To validate the accuracy of the DIC measurements under dynamic conditions using the high-speed imaging system, a random speckle pattern was applied at the end of a Kolsky bar apparatus shown in Figure 4. In a Kolsky bar experiment, the striker bar impacts the incident bar to generate a wave travelling through the incident bar. The wave is partially reflected and partially transmitted at the incident bar/ transmitted bar interface. Using the strain measurements of the pre-calibrated strain gages mounted on the incident and transmitted bars, the velocity at the end of

the transmitted bar can be calculated using eq. 2 below.

$$v(t)_{end} = 2\varepsilon(t)c_b \tag{2}$$

where v is the velocity at the end of the bar, ε is the strain measured at the gage, and c_b the wave speed of the bar. Integrating these velocities with time gives displacements, which are then compared with the DIC measurements. The results (Figure 5) showed good agreement between displacement measurements of the Kolsky bar setup and those obtained from DIC. The average percentage error was 3.35% for measurements up to 2 mm.

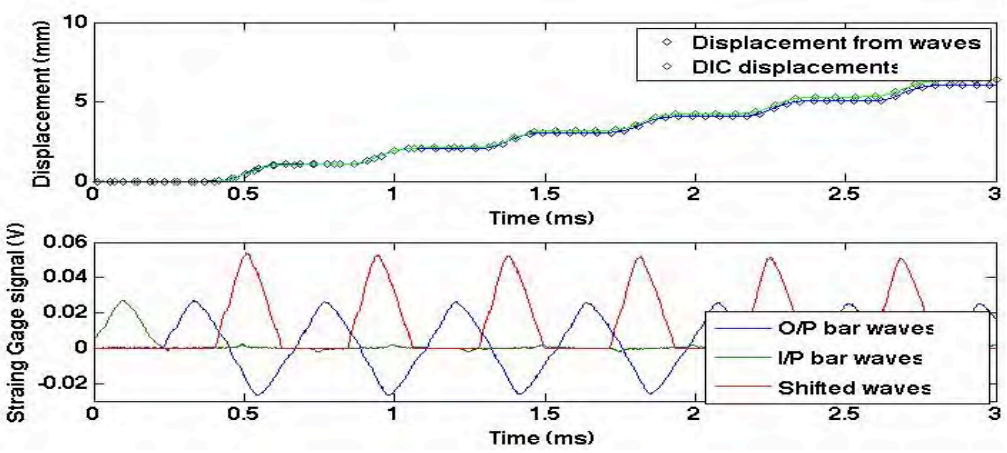

Figure 5: Results of Dynamic validation of DIC setup

2.1.3 Dynamic inflation test on bovine cornea:

Figure 6 superimposes plots of pressure (red) and displacement (blue) time-history measured for a preliminary inflation test performed on a bovine cornea sample. Also shown is a DIC reconstruction of the deformed surface of the specimen at the peak pressure. The pressure measurements were made about 5" away from the specimen. The pressure-displacement measurements were not synchronized for the experiment. An algorithm was developed to synchronize the pressure and displacement measurements and one of the pressure gages was placed closer to the tissues to provide a more accurate measurement of the pressure loading of specimen.

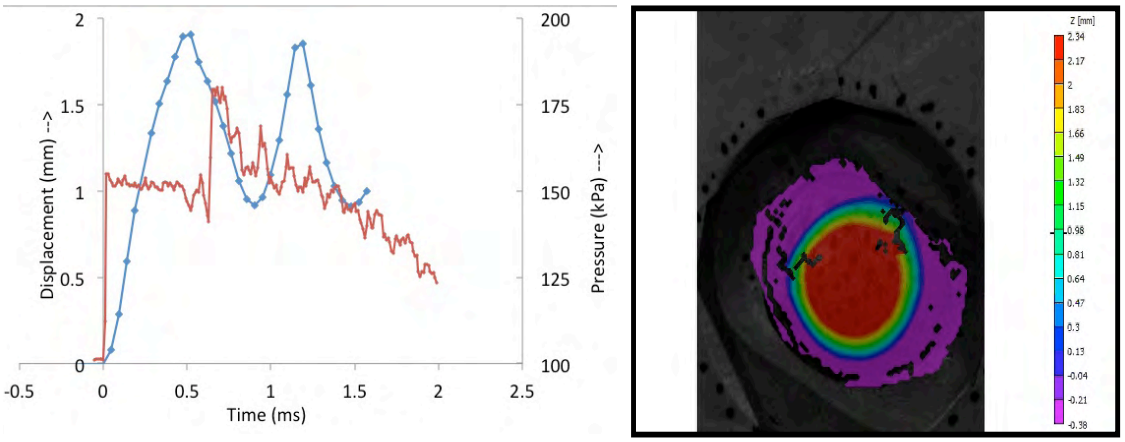

Figure 6: Results from a dynamic validation test on bovine cornea.

2.2 Feasibility Test for Composite Membrane Inflation

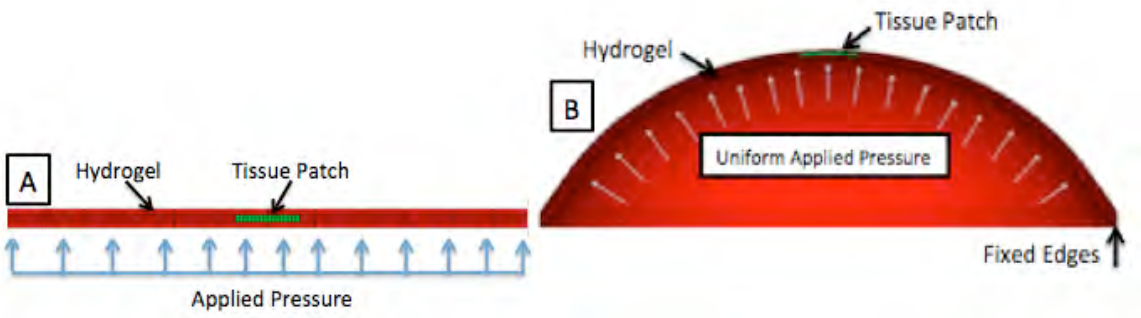

Figure 7. A finite element model of a composite hydrogel-tissue membrane. In simulation, this membrane is inflated from a flat position (A) to a uniformly inflated membrane (B).

We developed a computational model to investigate the feasibility of a planned novel composite membrane inflation test to measure the stress-strain response of the cornea and sclera. The test would require encapsulating a small tissue patch (e.g. cornea or sclera) within a hydrogel membrane and fully fixing the edges of the hydrogel membrane to the end of a shock tube. The inflation test measures the displacement field of the specimen surface, which is used to calculate the strain experienced by the inflating membrane. The tensile hoop stresses in the membrane are typically calculated from the applied pressure (P), the radius of curvature (R), and thickness of the membrane (t) using Laplace's law:

$$\sigma_{\theta\theta} = \frac{pR}{2t} \tag{3}$$

This analysis neglects the effects of bending and assumes that the stresses do not vary through the thickness. We developed a finite element model of the tissue-hydrogel composite membrane subjected to a controlled pressurization (Fig. 6) to investigate the validity of applying Laplace's law to calculate the stresses in the membrane in the presence of material non-linearity (of the tissue) and membrane heterogeneity.

The results showed that the strain field exhibited a small (~10-15%) linear variation through the thickness because of bending. The small strain variation caused a large stress variation (~200%) through the thickness because of the mismatch in materials properties of the hydrogel and tissues and because of material nonlinearity (Figure 8).

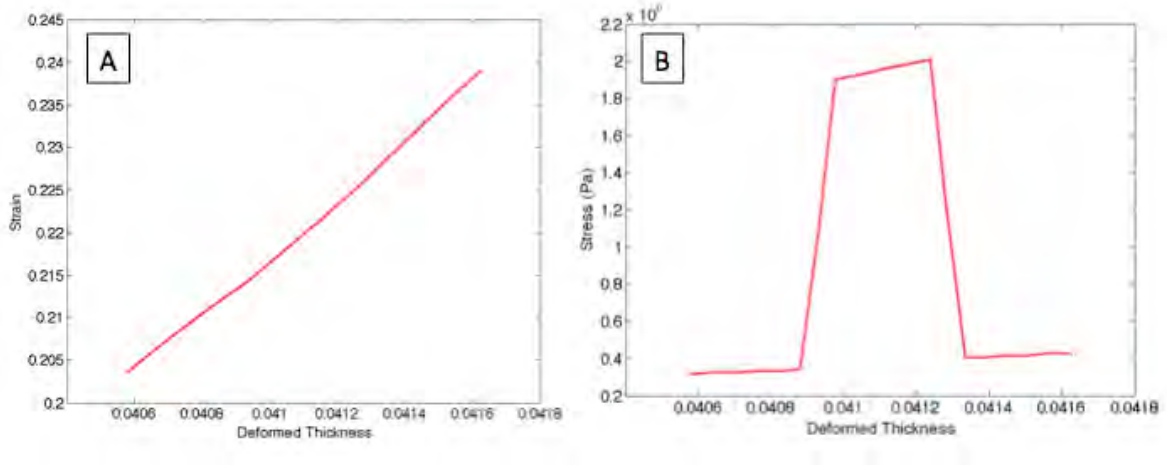

Figure 8. (A) The strain varies linearly through the thickness of the composite membrane (~10-15% strain gradient). (B) The stress is discontinuous through the thickness of the composite membrane, due to both material nonlinearity and a mismatch in material properties of the hydrogel and tissue.

The modeling study revealed that Laplace's law accurately calculated the stress resultant (stress integrated through the thickness),

$$N = \int_{-t/2}^{t/2} \sigma \, dz = \frac{PR}{2} \tag{4}$$

even for the case of large material nonlinearities and heterogeneity. Based on these findings, we developed a method for determining the mechanical properties of the

tissues from the inflation test data. In the method, the DIC measured displacements are used to calculate the circumferential strains and curvature of the inflated membrane. The curvature is used to calculate the stress resultant *N* which is related to the circumferential stress through eq. (4). The material properties of a stress (σ)-strain model can be fitted to the stress resultant (*N*) – strain data by assuming a linear strain variation through the thickness as follows:

$$\lambda_o = \lambda_m + Kz \tag{5}$$

where is the stretch at the outer surface of the membrane, is the stretch at the midplane, K is the curvature at the midplane, and z is the distance from the midplane to the outer surface

2.3 Constitutive Model

We are developing a theoretical model for the stress-strain response of the cornea and sclera that incorporates the effects of the anisotropic arrangement of the collagen lamellae and the crimped structure of the collagen fibril. The former gives rise to the anisotropic response while the crimped fibril structure provides the J-shaped stiffening stress-strain response. Figure 9 illustrates the fibrous microstructure of the cornea (6). The cornea is composed of approximately 250 lamellae of collagen fibrils. The fibrils within one lamella run parallel to one another, but subtend large angles between adjacent lamellae (7). In a relaxed state, the collagen fibrils within the lamella assume a crimped shape. When the tissue is stretched, the fibrils are first un-crimped (straightened) without stretching. Further stretching of the tissue at the macro-scale causes the fibrils themselves to be stretched at the micro-scale. This behavior describes the tissue's nonlinearity (8).

The constitutive relation is developed from a strain energy potential. The strain energy of the tissue will be divided into a matrix, a fiber, and a fiber-fiber interaction component. The matrix of the tissue will be modeled as an isotropic, hyperelastic material. The fiber component, which is a multiplicative decomposition of the energy of the fibril at the micro-scale and the fiber orientation distribution function, describes the anisotropy of the tissue. At the micro-scale, the

fibril behavior describes the nonlinearity of the tissue. As the tissue is stretched the fibers also interact with adjacent fibers, and under dynamic loads, this interaction will exhibit rate-dependence, and therefore be modeled as a viscoelastic component.

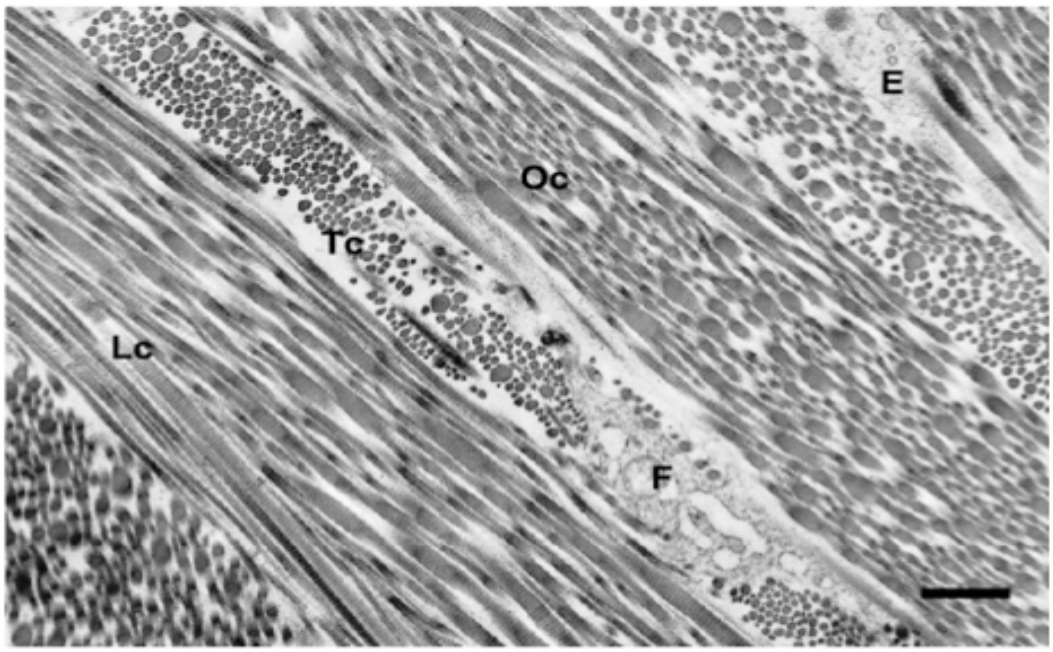

Figure 9. Electron micrograph of scleral tissue showing lamellar structure. Collagen fibrils are shown in the longitudinal (Lc), transverse (Tc) and oblique (Oc) directions within the lamella.

2.4 Computational Model of the Globe

To date, a finite element model of the corneo-scleral shell, taking into account the variation in thickness across the shell, has been developed (Figure 10A). Wide-Angle X-Ray Scattering (WAXS) data of collagen molecules of the human corneal and scleral tissues has been obtained during a recent visit to the Diamond Light Source in the UK's National Synchrotron Science Facility (Figure 10B). This data will soon be incorporated into the finite element model of the corneo-scleral shell, adding fiber orientations to capture the anisotropic behavior of the tissue.

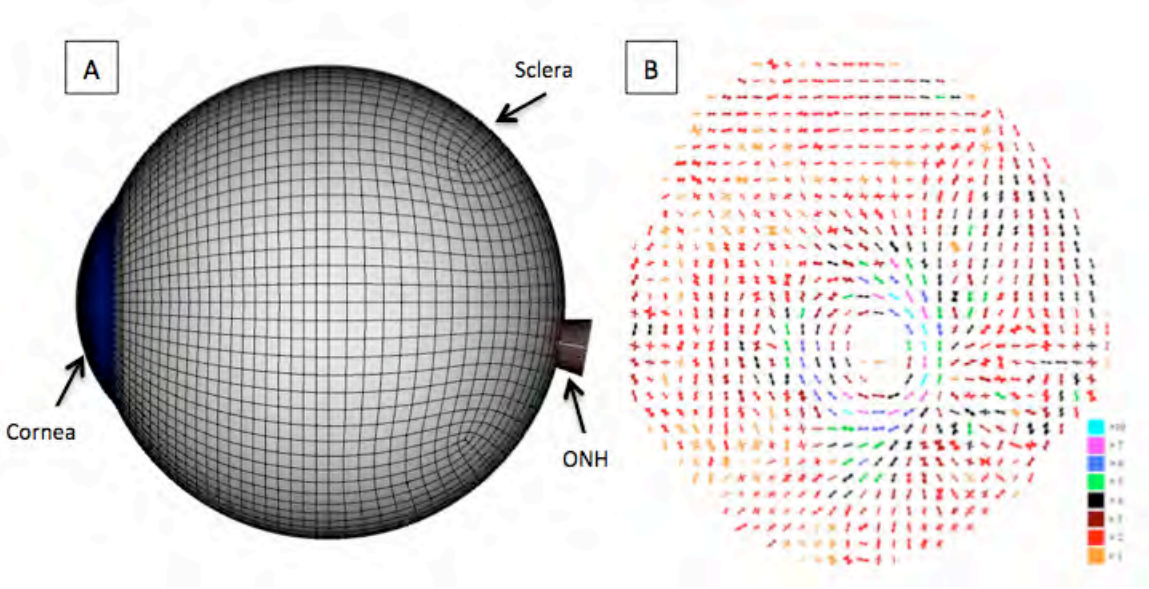

Figure 10. (A) A finite element model of the corneo-scleral shell, including the optic nerve head (ONH), consisting of linear hexahedral elements. (B) WAXS data of the collagen molecules within the peripheral scleral tissue shows the preferential orientation of the collagen lamella as individual polar plots. The color of each polar plot shows the degree of dispersion at the specific location.

3.0 KEY RESEARCH OUTCOMES

1. Built a shock tube system with digital image correlation (DIC) setup to perform dynamic inflation experiments of ocular tissues and blast experiments on the globe.
2. Validated the shock-tube design by comparing theoretical and measured shock pressures.
3. Measured the accuracy of the DIC displacement measurements for both quasi-static and dynamic test systems.
4. Obtained Bio-Safety Level 2 certification for the shock tube experimental facilities.
5. Performed a preliminary dynamic inflation experiment on bovine cornea.
6. Performed a modeling study of the feasibility of using an innovative composite membrane inflation test method to characterize the mechanical properties of ocular tissues. Results showed that Laplace's law can be used

to calculate the stress resultant of the composite membrane when the tissue patch is up to 3 times stiffer than the encapsulating hydrogel.

7. Developed a finite element model of the human corneo-scleral shell that incorporates experimentally measured regional variations of the tissue's thickness.
8. Began developing a microstructure-based constitutive model to describe the nonlinear, anisotropic stress response of the tissues.
9. Developed a finite element model of the human corneo-scleral shell with regional thickness variation.
10. Measured the anisotropic collagen orientation distribution of the posterior human sclera.

4.0 Reportable Outcomes

1. Poster Presentation (SBC2011-53997): Summer Bioengineering Conference, June 22-25th, 2011, Farmington Pennsylvania
   Ziegler K.A., Yatnalkar R.S., Ramesh K.T., Nguyen T.D. "*Modeling Study for the Design of An Innovative Composite Membrane Inflation Test".*

2. Conference presentation: Society of Experimental Mechanics,
   June 11-14th, 2011, Uncasville, CT.
   Yatnalkar R.S., Ziegler K.A., Ramesh K.T., Nguyen T.D., "Development of a shock tube to study primary blast effects in ocular blast injuries".

3. Kimberly Ziegler received the Science, Mathematics And Research for Transformation (SMART) Scholarship for Service Program, established by the Department of Defense (DoD), which provides full funding for FY12-FY15.

5.0 CONCLUSION

The main focus over the first year of the project was to develop an innovative dynamic inflation test method for characterizing the behavior of the cornea and sclera at dynamic loading rates. A shock tube test system with digital image correlation was developed and validated. It is currently in the stages of preliminary testing. From a computational standpoint, the main goal was to develop a method for calculating the stress and strain fields from the applied pressure and measured displacement field, and a modeling study verifying the design of these inflation tests. These accomplishments adds to the scientific knowledge base for ocular biomechanics under blast conditions

For FY12, the experimental effort will focus on applying the shock tube test system to measure the dynamic stress-strain response and rupture conditions of human cornea and sclera. For the modeling effort, we will complete development of a stress-strain model for the cornea and sclera that incorporates the anisotropic lamellar structure and crimped fibril structure. The parameters of the model will be determined from the inflation measurements. The stress-strain relation is needed for finite element simulations of blast loading of the globe. The finite element model of the corneo-scleral shell will be extended to include the lens to provide the barrier between the anterior and posterior chamber of the globe. A fluid-structure interaction solver (FSI) will be developed to simulate primary blast loading at the globe and head level. This solver couples a sharp-interface immersed boundary method [9] for flow simulation with in-house finite-element based structure dynamics solver Tahoe. This solver will be used in conjunction with the experiments and the following work is planned at different levels. At the globe level, internal blast wave propagation through the aqueous humor, lens and vitreous humor will be characterized by the hotspots of internal stresses, time-history of intraocular pressure and the deformation response of globe to the blast wave. Transient deformation in the shape of the vitreous cavity are likely to have a large effect on the flow and pressure in the vitreous humor, which is not fully understood [10]. At the head level, blast wave reflections on the eye due to face and protective eye gear, and

influence of clearance gap between the eye and protective eyewear will be evaluated. This will allow us to assess the performance of standard issue eye protection. A recent study on the blast wave impact on skull has shown that a threshold clearance gap between the helmet and the head amplifies the pressures acting directly on the skull [11]. Simulations will also help to design next generation protective eyewear, which could drastically mitigate blast injuries.

6.0 REFERENCES

[1] J. K. Wright, 'Shock tubes', John Wiley and Sons, 1961.

[2] Michael A. Sutton et al., "Image Correlation for Shape, Motion and Deformation Measurements, Basic concepts, Theory and Applications," Springer, 2009.

[3] V. Tiwari et al., "Assessment of High Speed Imaging Systems for 2D and 3D Deformation Measurements: Methodology Development and Validation", Experimental Mechanics, Volume 47, Number 4, 561-579 .

[4] A. Gilat, T. Schmidt, and J. Tyson, "Full field strain measurement during a tensile split Hopkinson bar experiment," Journal De Physique. IV, vol. 134, pp. 687-692, 2006.

[5] Boyce et al., "Full field deformation of bovine cornea under constrained inflation conditions", Biomaterials, Volume 29, p 3896-3904, 2008.

[6] Watson, P.G., Young, R.D. Scleral structure, organisation and disease. A review. Experimental Eye Research 78 (2004) 609–623, 2004.

[7] Pinsky PM, D. van der Heide, and Chernyak D. Computational modeling of the mechanical anisotropy in the cornea and sclera. J. Cataract. Refract. Surg., 31:136–145, 2005.

[8] Grytz R and Meschke G. Constitutive framework for crimped collagen fibrils in soft tissues. Journal of Mechanical Behavior Biomedical Materials. Vol. 2, 522–533, 2008.

[9] Mittal, R., Dong, H, Bozkurttas, M., Najjar, F.M., Vargas, A. and von Loebbeck, A. A Versatile Immersed Boundary Methods for Incompressible Flows with Complex Boundaries. J. Comp. Phys. Vol. 2 27 (10), 2008.

[10] Siggers J.H. and Ethier C.R., Fluid Mechanics of the Eye, Annual Review of Fluid Mechanics, Vol 2011.

[11] Moss et al, Skull Flexure from Blast Waves: A Mechanism for Brain Injury with Implications for Helmet Design, Phy. Rev. Lett., Vol 103, 2009.